Cell Reports Medicine, Volume *3*

Supplemental information

Human early syncytiotrophoblasts are highly susceptible to SARS-CoV-2 infection

Degong Ruan, Zi-Wei Ye, Shuofeng Yuan, Zhuoxuan Li, Weiyu Zhang, Chon Phin Ong, Kaiming Tang, Timothy Theodore Ka Ki Tam, Jilong Guo, Yiyi Xuan, Yunying Huang, Qingqing Zhang, Cheuk-Lun Lee, Liming Lu, Philip C.N. Chiu, William S.B. Yeung, Fang Liu, Dong-Yan Jin, and Pentao Liu

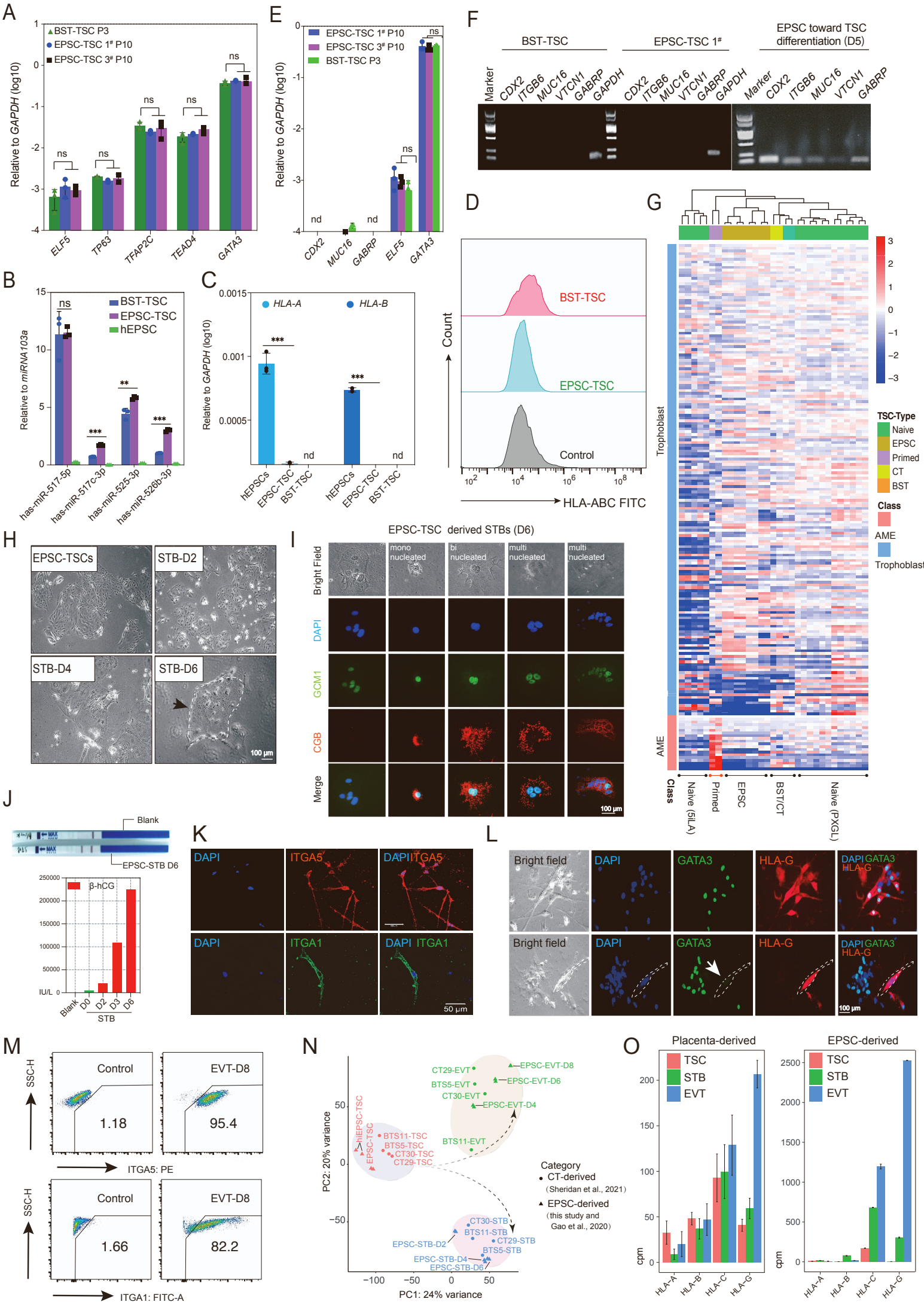
A
BST-TSC P3
EPSC-TSC 1# P10
EPSC-TSC 3# P10
Relative to GAPDH (log10)
ELF5
TP63
TFAP2C
TEAD4
GATA3
ns
E
EPSC-TSC 1# P10
EPSC-TSC 3# P10
BST-TSC P3
Relative to GAPDH (log10)
CDX2
MUC16
GABRP
ELF5
GATA3
nd
F
BST-TSC
EPSC-TSC 1#
EPSC toward TSC differentiation (D5)
Marker
CDX2
ITGB6
MUC16
VTCN1
GABRP
GAPDH
B
BST-TSC
EPSC-TSC
hEPSC
Relative to miRNA103a
has-miR-517-5p
has-miR-517c-3p
has-miR-525-3p
has-miR-526b-3p
C
HLA-A
HLA-B
Relative to GAPDH (log10)
hEPSCs
EPSC-TSC
BST-TSC
D
BST-TSC
EPSC-TSC
Control
Count
HLA-ABC FITC
G
Trophoblast
AME
TSC-Type
Naive
EPSC
Primed
CT
BST
Class
AME
Trophoblast
Naive (5iLA)
Primed
EPSC
BST/CT
Naive (PXGL)
H
EPSC-TSCs
STB-D2
STB-D4
STB-D6
100 μm
I
EPSC-TSC derived STBs (D6)
Bright Field
DAPI
GCM1
CGB
Merge
mono nucleated
bi nucleated
multi nucleated
multi nucleated
100 μm
J
Blank
EPSC-STB D6
β-hCG
IU/L
Blank
D0
D2
D3
D6
STB
K
DAPI
ITGA5
DAPI ITGA5
DAPI
ITGA1
DAPI ITGA1
50 μm
L
Bright field
DAPI
GATA3
HLA-G
DAPI GATA3 HLA-G
100 μm
M
Control
EVT-D8
1.18
95.4
SSC-H
ITGA5: PE
1.66
82.2
ITGA1: FITC-A
N
CT29-EVT
BTS5-EVT
CT30-EVT
BTS11-EVT
EPSC-EVT-D8
EPSC-EVT-D6
EPSC-EVT-D4
hiEPSC-TSC
EPSC-TSC
BTS11-TSC
BTS5-TSC
CT30-TSC
CT29-TSC
CT30-STB
BTS11-STB
CT29-STB
BTS5-STB
EPSC-STB-D2
EPSC-STB-D4
EPSC-STB-D6
PC2: 20% variance
PC1: 24% variance
Category
CT-derived
(Sheridan et al., 2021)
EPSC-derived
(this study and Gao et al., 2020)
O
Placenta-derived
EPSC-derived
TSC
STB
EVT
cpm
HLA-A
HLA-B
HLA-C
HLA-G

Figure S1. Generating trophoblast stem cells (TSCs) and subtype trophoblasts from hEPSCs. Related to Figure 1. RT-qPCR analysis of trophoblast genes (A) trophoblast-specific C19MC miRNAs (B), *HLA-A* and *-B* (C), and *CDX2* and putative AME genes (E) were performed in hEPSCs and/or EPSC-TSCs and BST-TSC. Results are normalized to levels of *GAPDH* for marker genes or *miR-103a* for miRNAs using the ΔCt method Data are mean ± sd, n=3 biological replicates. Student's *t*-test, nd: not detectable, ns: not significant, ** $P < 0.01$; *** $P < 0.001$; (D) Flow cytometry quantification of HLA-A, B, C on EPSC-TSCs and BST-TSCs. The antibody isotype is the control. (F) RT-PCR detection of *CDX2* and putative AME genes in EPSC-TSCs, BST-TSC, and in cells of hEPSCs differentiation toward hTSCs on day 5. (G) Heatmap for signature genes of trophoblast and AME (Table S1). Genes are ordered by expression in respective gene sets and samples are ordered by cluster result. Expression is normalized with mean and log2 transformed. (H) Representative bright field images of STBs generated from EPSC-TSCs on day 2, 4 and 6. The arrow points to a multinucleated STB circled by a dashed line. Scale bar: 100 μm (I) STBs generated from EPSC-TSCs have distinct morphologies (mono-, bi- or multinucleated) and express GCM1 and CGB. Scale bar: 100 μm (J) Upper panel: Representative results using a human pregnancy test strip on medium collected from day-6 EPSC-STBs and STB medium control (Blank). Lower panel: ELISA (IU/L) detection of β-hCG in supernatant from different STB differentiation timepoints as indicated. (K) Immunofluorescence staining (ITGA1 and ITGA5) of day8 EVTs generated from EPSC-TSCs. Scale bar: 100 or 50 μm as indicated (L) EVTs generated from EPSC-TSCs (day 8) are immunofluorescence stained for GATA3 and HLA-G. Arrow indicates that a mature EVT (spindle shape, circled by a dashed line) does not express high GATA3. Scale bar: 100 μm (M) Flow cytometry quantification of EVT marker ITGA5 and ITGA1 on EVTs differentiated from EPSC-TSCs (day 8). (N) PCA analysis for comparison of placenta-derived trophoblast cells (CT and BTS) and EPSC-derived trophoblast cells (EPSC-TSC; EPSC-TSC differentiating toward STB at day2, 4, 6, and toward EVT at day4, 6 and 8, respectively). (O) Expression of HLA genes in human placenta-derived trophoblasts and EPSC-TSCs and their derivative trophoblasts. Error bars: standard errors.

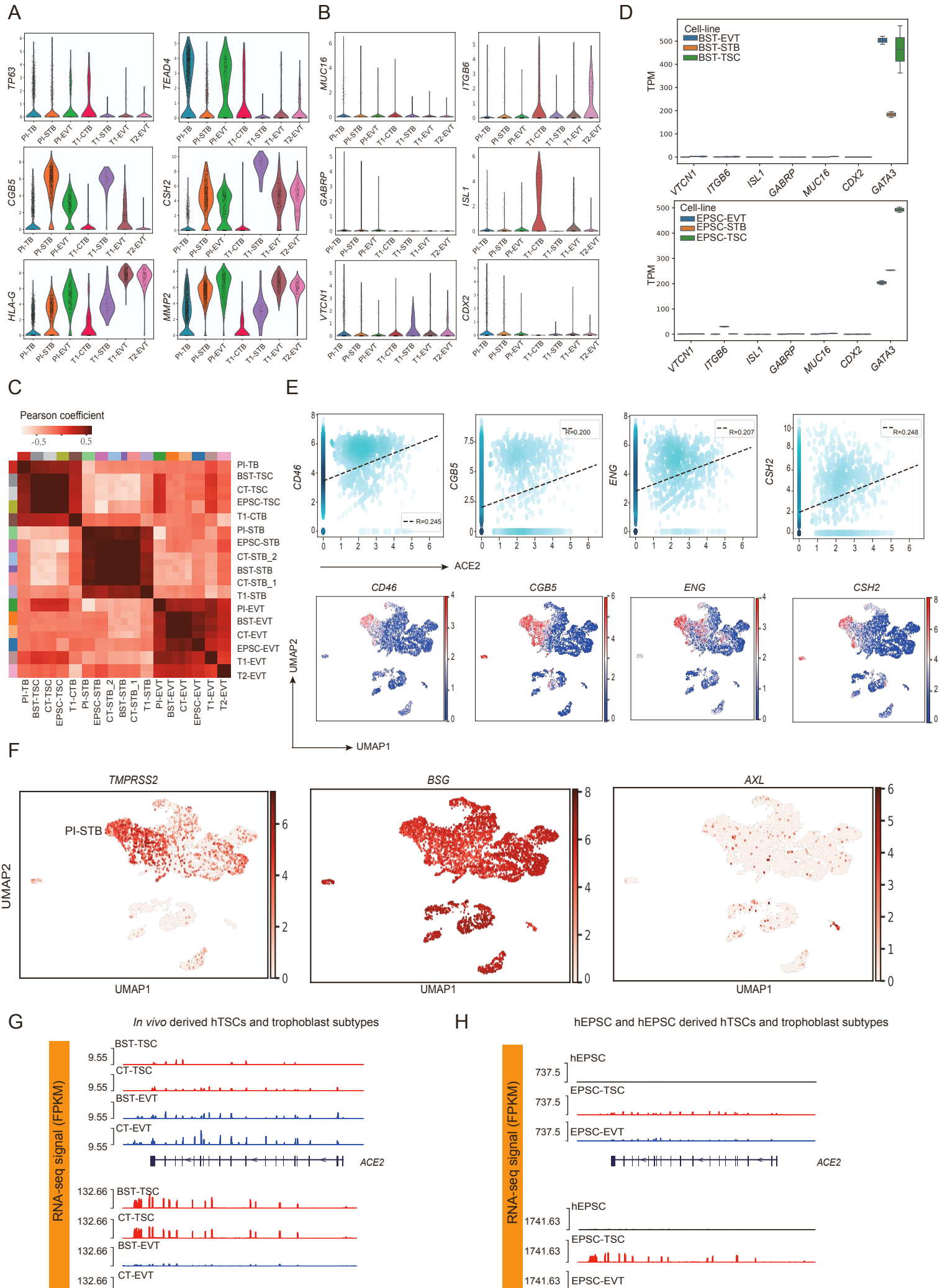
A
TP63
TEAD4
CGB5
CSH2
HLA-G
MMP2
B
MUC16
ITGB6
GABRP
ISL1
VTCN1
CDX2
PI-TB
PI-STB
PI-EVT
T1-CTB
T1-STB
T1-EVT
T2-EVT
D
Cell-line
BST-EVT
BST-STB
BST-TSC
EPSC-EVT
EPSC-STB
EPSC-TSC
TPM
VTCN1
ITGB6
ISL1
GABRP
MUC16
CDX2
GATA3
C
Pearson coefficient
-0.5
0.5
PI-TB
BST-TSC
CT-TSC
EPSC-TSC
T1-CTB
PI-STB
EPSC-STB
CT-STB_2
BST-STB
CT-STB_1
T1-STB
PI-EVT
BST-EVT
CT-EVT
EPSC-EVT
T1-EVT
T2-EVT
E
CD46
CGB5
ENG
CSH2
R=0.245
R=0.200
R=0.207
R=0.248
ACE2
UMAP2
UMAP1
F
TMPRSS2
BSG
AXL
PI-STB
UMAP2
UMAP1
G
In vivo derived hTSCs and trophoblast subtypes
RNA-seq signal (FPKM)
BST-TSC
CT-TSC
BST-EVT
CT-EVT
9.55
132.66
ACE2
TMPRSS2
H
hEPSC and hEPSC derived hTSCs and trophoblast subtypes
hEPSC
EPSC-TSC
EPSC-EVT
737.5
1741.63

Figure S2. Trophoblasts derived from hEPSCs resemble those in human peri-implantation embryos and the placenta. Related to Figure 2. Violin plots showing log-transformed TPM of trophoblast genes (A) and putative AME genes (B) in human peri-implantation embryos and placenta trophoblasts. (C) Heatmap of Pearson correlation coefficients among transcriptomics of peri-implantation embryo and placenta (pseudo-bulk RNAseq), and the *in vitro* cultured trophoblasts (bulk RNAseq). Batch effects were regressed out in transcriptomic expression. *In vitro* trophoblast samples include blastocyst- and placenta-derived TSCs (BST-TSC, CT-TSC) and the trophoblast subtypes STBs (BST-STB, CT-STB) and EVTs (BST-EVT, CT-EVT), and EPSC-TSC and their trophoblast subtypes STBs and EVTs (EPSC-STB, EPSC-EVT). (D) Potential amnion marker expression (in TPM) in hTSC derived from the blastocyst (BST, Upper panel) and hEPSC (Bottom panel) and their derivatives. *GATA3* is a non-amnion marker for comparison. (E) Upper panel: Scatter plots showing the positive Pearson correlations of *CD46*, *CGB5*, *ENG* and *CSH2* with *ACE2* expression. Linear regression is drawn in black dashed line. The darkness of blue indicates cell density. Lower panel: Scaled expression of STB genes in human peri-implantation embryo and placenta trophoblasts. (F) Scaled expression of *TMPRSS2*, *BSG* and *AXL* in human peri-implantation embryo and placenta trophoblasts. (G-H) RNA-seq signal of *ACE2* and *TMPRSS2* in *in vivo* derived trophoblasts (G) and in hEPSCs and hEPSC derivatives (H). *ACE2* and *TMPRSS2* genomic regions are plotted at the bottom, where each vertical bar represents an exon.

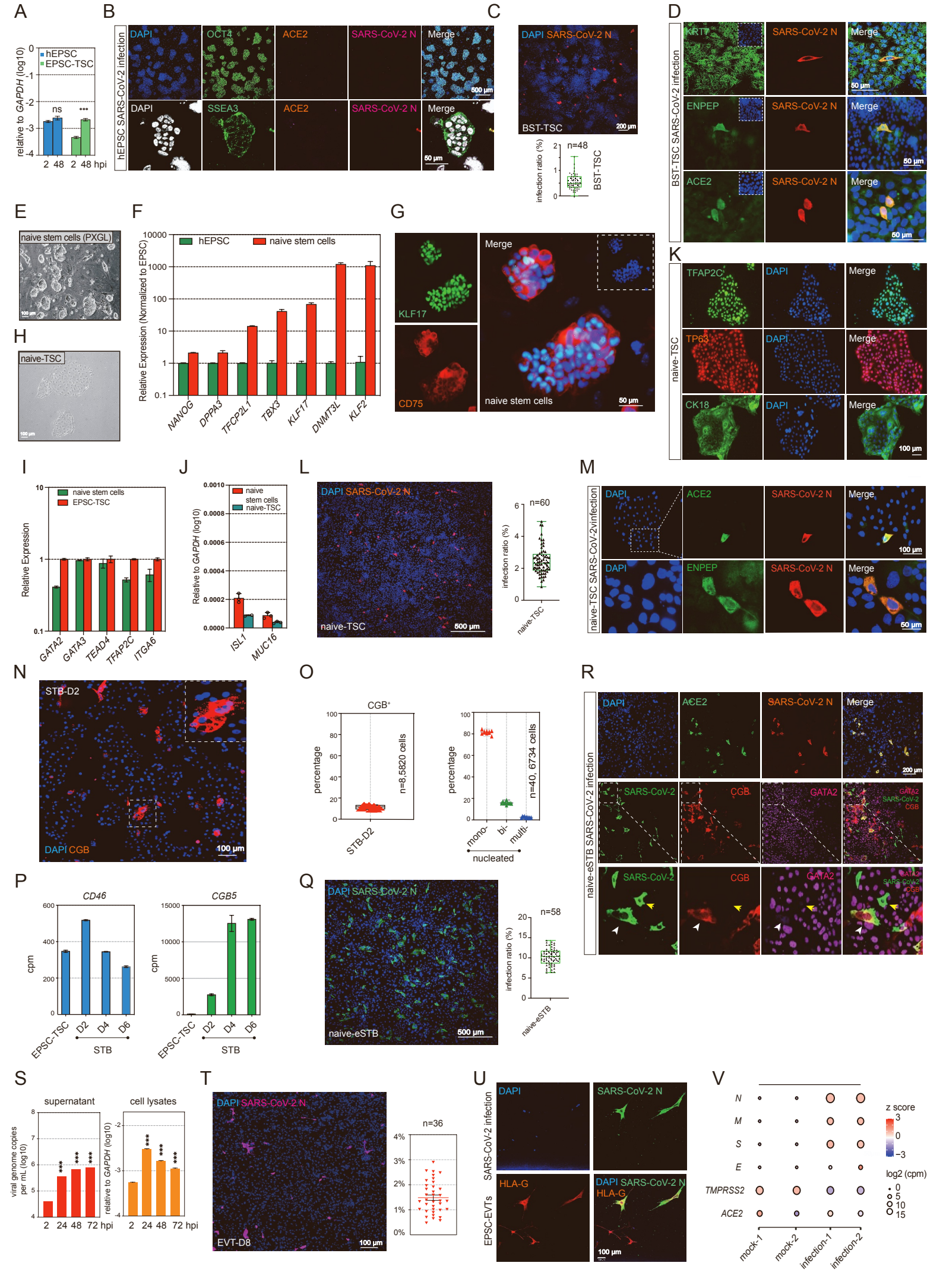
A
relative to GAPDH (log10)
hEPSC
EPSC-TSC
ns
***
2 48 2 48 hpi
B
hEPSC SARS-CoV-2 infection
DAPI
OCT4
ACE2
SARS-CoV-2 N
Merge
SSEA3
50 μm
C
DAPI SARS-CoV-2 N
BST-TSC
200 μm
infection ratio (%)
n=48
BST-TSC
D
BST-TSC SARS-CoV-2 infection
KRT7
ENPEP
ACE2
50 μm
E
naive stem cells (PXGL)
100 μm
F
Relative Expression (Normalized to EPSC)
hEPSC
naive stem cells
NANOG
DPPA3
TFCP2L1
TBX3
KLF17
DNMT3L
KLF2
G
KLF17
CD75
Merge
naive stem cells
50 μm
H
naive-TSC
100 μm
K
naive-TSC
TFAP2C
TP63
CK18
DAPI
100 μm
I
Relative Expression
naive stem cells
EPSC-TSC
GATA2
GATA3
TEAD4
TFAP2C
ITGA6
J
Relative to GAPDH (log10)
naive stem cells
naive-TSC
ISL1
MUC16
L
DAPI SARS-CoV-2 N
naive-TSC
500 μm
infection ratio (%)
n=60
naive-TSC
M
naive-TSC SARS-CoV-2vinfection
DAPI
ACE2
SARS-CoV-2 N
Merge
ENPEP
100 μm
50 μm
N
STB-D2
DAPI CGB
100 μm
O
CGB+
percentage
n=8,5820 cells
STB-D2
n=40, 6734 cells
mono-
bi-
multi-
nucleated
R
naive-eSTB SARS-CoV-2 infection
DAPI
ACE2
SARS-CoV-2 N
Merge
200 μm
SARS-CoV-2
CGB
GATA2
P
CD46
CGB5
cpm
EPSC-TSC
D2
D4
D6
STB
Q
DAPI SARS-CoV-2 N
naive-eSTB
500 μm
infection ratio (%)
n=58
naive-eSTB
S
supernatant
cell lysates
viral genome copies per mL (log10)
relative to GAPDH (log10)
2 24 48 72 hpi
T
DAPI SARS-CoV-2 N
EVT-D8
100 μm
n=36
U
SARS-CoV-2 infection
EPSC-EVTs
DAPI
SARS-CoV-2 N
HLA-G
100 μm
V
N
M
S
E
TMPRSS2
ACE2
mock-1
mock-2
infection-1
infection-2
z score
log2 (cpm)

Figure S3. *In vitro* generated human trophoblasts are susceptible to SARS-CoV-2 infection. Related to Figure 3. (A) RT-qPCR detection of SARS-CoV-2 genome copy number in cell lysates of 2 h.p.i. and 48 h.p.i hEPSCs and EPSC-TSCs. (B) Immunofluorescence staining of 48 h.p.i. hEPSCs for pluripotent markers OCT4 or SSEA3 and ACE2, SARS-CoV-2 N protein. Scale bar: 100 μm. (C) Immunofluorescence-stained 24 h.p.i. BST-TSCs for SARS-CoV-2 N protein. Scale bar: 100 μm. Lower panel: Percentages of SARS-CoV-2 N protein positive BST-TSCs. n=48 random immunofluorescence staining images. (D) Immunofluorescence-stained SARS-CoV-2 N protein, ACE2, ENPEP, and KRT7 in 24 h.p.i. BST-TSC. Scale bar: 50 μm (E) Phase-contrast image of human naïve stem cells (H1) cultured on MEFs in PXGL condition. Scale bar: 100 μm (F) RT-qPCR quantification of naïve marker gene expression in naïve stem cells compared to hEPSCs (mean ± s.d. n=3). (G) Immunofluorescence staining of naïve pluripotency markers KLF17 and CD75 in naïve stem cells. Scale bar: 50 μm. (H) Phase-contrast image of naïve stem cell-derived hTSCs (naïve-TSCs). Scale bar: 100 μm (I) RT-qPCR quantification of hTSC marker gene expression in naïve-TSC compared to EPSC-TSC (mean ± s.d. n=3). (J) RT-qPCR quantification of *ISL1* and *MUC16* gene expression in naïve stem cells and naive-TSCs (mean ± s.d. n=3). (K) Immunofluorescence staining of hTSC markers in naïve-TSCs. Scale bar: 50 μm. (L) Immunofluorescence staining of SARS-CoV-2 N protein in 24 h.p.i. naïve-TSCs. Scale bar: 500 μm. Right panel: Percentages of SARS-CoV-2 N protein positive naïve-TSCs, respectively. n=60 random images. (M) Immunofluorescence staining of ENPEP and ACE2, SARS-CoV-2 N protein and in 24 h.p.i. naïve-TSCs. Scale bar: 100 μm and 50 μm as indicated. (N) Immunofluorescence staining for CGB in STB-D2. Dotted box showed a multinucleated CGB^+ cells. Scale bar: 100 μm. (O) Quantification of the percentages of CGB^+ in STB-D2. Error bar, mean and standard error (SEM). n=8 random images, total 5820 cells. Right panel: Quantification of percentages of mono-, bi- and multi-nucleated cells in STB-D2. Error bar, mean and standard error (SEM). n=40 random images, total 6734 cells. (P) RNAseq analysis of expression of *CD46* and *CGB5* in EPSC-TSCs and different STB differentiation timepoints. (Q) Representative immunofluorescence staining of 24 h.p.i. naïve-eSTB for SARS-CoV-2 N protein. Scale bar: 500 μm. Right panel: Percentages of SARS-CoV-2 N protein positive naïve-eSTBs, respectively. n=58 random images. (R) Immunofluorescence staining of 24 h.p.i. naïve-eSTB for ACE2, SARS-CoV-2 N protein, GATA2 and CGB. Dotted box showed mononucleated and binucleated infected naïve-eSTBs, some of them (white arrows) start to express CGB. Scale bar: 200 μm. (S) RT-qPCR analysis of SARS-CoV-2 genome copy number in supernatants and cell lysates of 2, 24, 48 and 72 h.p.i. EVTs (day8). Data are mean ± s.d. n=3 biological replicates. Student's *t*-test, *** $P < 0.001$ (T) Immunofluorescence staining of 48 h.p.i. EVTs for SARS-CoV-2 N protein. Scale bar: 100 μm. Right panel: Percentages of SARS-CoV-2 N protein positive EVTs. n=36 random images. (U) Immunofluorescence-stained SARS-CoV-2 infected EVTs for N protein and HLA-G. Scale bar: 100 μm (V) Bubble plot for *ACE2*, *TMPRSS2* and genes of SARS-CoV-2 expression in 48 h.p.i. mock and infected EVTs. Label color is according to z-score and bubble sizes are proportional to expression levels.

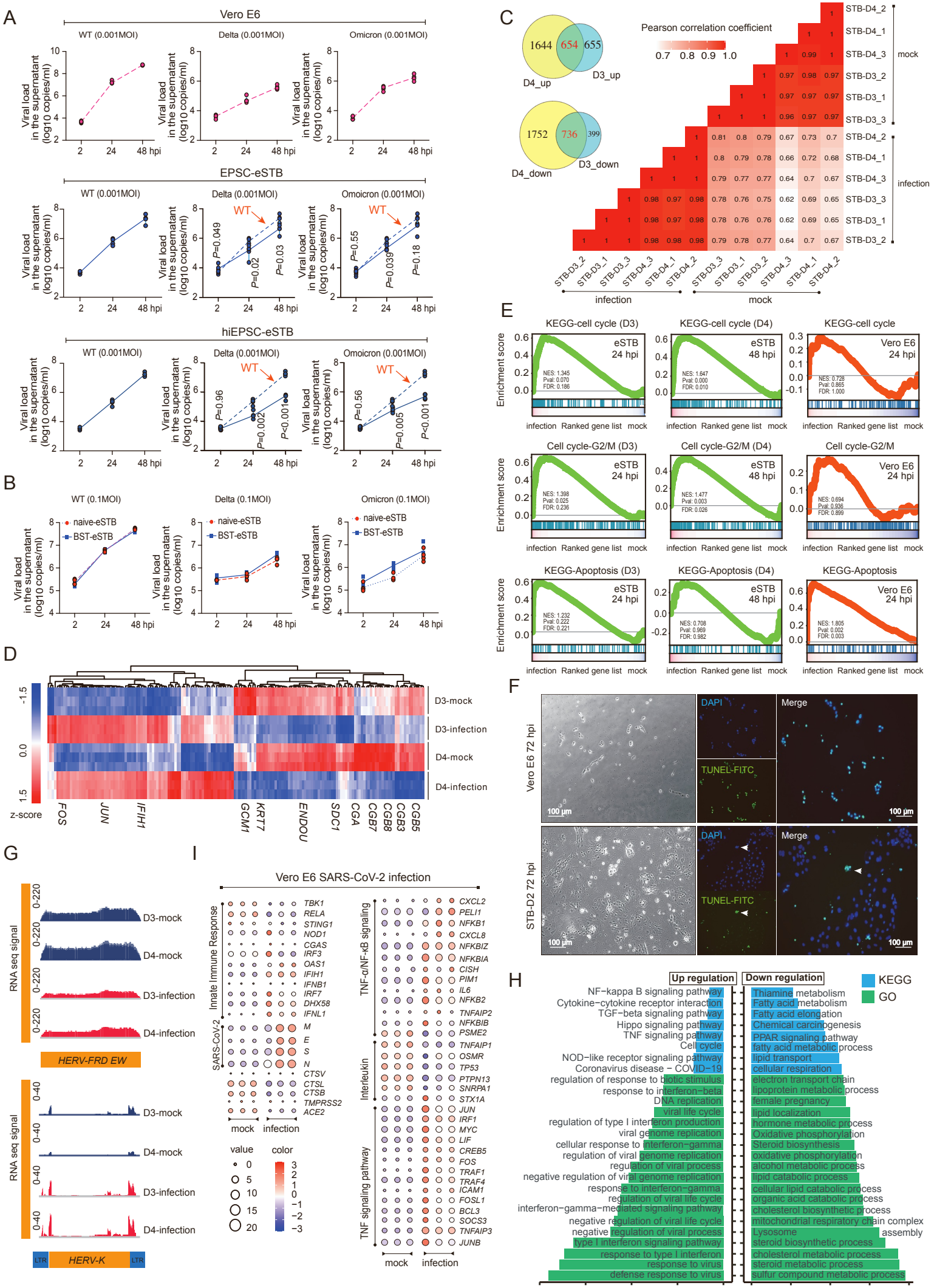
A
Vero E6
WT (0.001MOI)
Delta (0.001MOI)
Omicron (0.001MOI)
EPSC-eSTB
Omoicron (0.001MOI)
hiEPSC-eSTB
Viral load in the supernatant (log10 copies/ml)
2
24
48 hpi
WT
P=0.049
P=0.02
P=0.03
P=0.55
P=0.039
P=0.18
P=0.96
P=0.002
P<0.001
P=0.56
P=0.005
P<0.001
B
WT (0.1MOI)
Delta (0.1MOI)
Omicron (0.1MOI)
naive-eSTB
BST-eSTB
C
1644
654
655
D4_up
D3_up
1752
736
399
D4_down
D3_down
Pearson correlation coefficient
0.7 0.8 0.9 1.0
STB-D4_2
STB-D4_1
STB-D4_3
STB-D3_2
STB-D3_1
STB-D3_3
mock
infection
D
-1.5
0.0
1.5
z-score
D3-mock
D3-infection
D4-mock
D4-infection
FOS
JUN
IFIH1
GCM1
KRT7
ENDOU
SDC1
CGA
CGB7
CGB8
CGB3
CGB5
E
KEGG-cell cycle (D3)
KEGG-cell cycle (D4)
KEGG-cell cycle
Cell cycle-G2/M (D3)
Cell cycle-G2/M (D4)
Cell cycle-G2/M
KEGG-Apoptosis (D3)
KEGG-Apoptosis (D4)
KEGG-Apoptosis
Enrichment score
eSTB 24 hpi
eSTB 48 hpi
Vero E6 24 hpi
Ranked gene list
F
Vero E6 72 hpi
STB-D2 72 hpi
DAPI
TUNEL-FITC
Merge
100 μm
G
RNA seq signal
D3-mock
D4-mock
D3-infection
D4-infection
HERV-FRD EW
HERV-K
LTR
I
Vero E6 SARS-CoV-2 infection
Innate Immune Response
SARS-CoV-2
TNF-α/NF-κB signaling
Interleukin
TNF signaling pathway
TBK1
RELA
STING1
NOD1
CGAS
IRF3
OAS1
IFIH1
IFNB1
IRF7
DHX58
IFNL1
M
E
S
N
CTSV
CTSL
CTSB
TMPRSS2
ACE2
CXCL2
PELI1
NFKB1
CXCL8
NFKBIZ
NFKBIA
CISH
PIM1
IL6
NFKB2
TNFAIP2
NFKBIB
PSME2
TNFAIP1
OSMR
TP53
PTPN13
SNRPA1
STX1A
JUN
IRF1
MYC
LIF
CREB5
FOS
TRAF1
TRAF4
ICAM1
FOSL1
BCL3
SOCS3
TNFAIP3
JUNB
mock
infection
value
color
H
Up regulation
Down regulation
KEGG
GO
NF−kappa B signaling pathway
Cytokine−cytokine receptor interaction
TGF−beta signaling pathway
Hippo signaling pathway
TNF signaling pathway
Cell cycle
NOD−like receptor signaling pathway
Coronavirus disease − COVID−19
regulation of response to biotic stimulus
response to interferon−beta
DNA replication
viral life cycle
regulation of type I interferon production
viral genome replication
cellular response to interferon−gamma
regulation of viral genome replication
regulation of viral process
negative regulation of viral genome replication
response to interferon−gamma
regulation of viral life cycle
interferon−gamma−mediated signaling pathway
negative regulation of viral life cycle
negative regulation of viral process
type I interferon signaling pathway
response to type I interferon
response to virus
defense response to virus
Thiamine metabolism
Fatty acid metabolism
Fatty acid elongation
Chemical carcinogenesis
PPAR signaling pathway
fatty acid metabolic process
lipid transport
cellular respiration
electron transport chain
lipoprotein metabolic process
female pregnancy
lipid localization
hormone metabolic process
Oxidative phosphorylation
Steroid biosynthesis
oxidative phosphorylation
alcohol metabolic process
lipid catabolic process
cellular lipid catabolic process
organic acid catabolic process
cholesterol biosynthetic process
mitochondrial respiratory chain complex
Lysosome
assembly
steroid biosynthetic process
cholesterol metabolic process
steroid metabolic process
sulfur compound metabolic process
-log10 (P value)

Figure S4. eSTB's susceptibility to SARS-CoV-2 variants and their differentiation impairment. Related to Figure 4. (A) Comparison of SARS-CoV-2 replication kinetics among Vero E6, EPSC-eSTB and hiEPSC-eSTB cells. Cells were infected with WT, the Delta variant or Omicron variant at 0.001MOI. Cell culture supernatant were collected at the indicated time-points and subject to viral load detection using RT-qPCR method. Data are mean ± s.d. n=3. Student's *t*-test, exact *P* values are presented. (B) Comparison of SARS-CoV-2 replication kinetics in naïve-eSTB and BST-eSTB cells. (C) Left panel: Venn plots for differential genes after SARS-CoV-2 WT infection in STB-D3 and STB-D4. Right panel: Heatmap for correlation between infected STBs and mock infection STBs. (D) The top 50 up or down-regulated genes in STB after virus infection. Genes are sorted by -log10 (p value). Z-score of log2 transformed cpm was used. Red, upregulated genes; blue, downregulated genes. (E) Gene set enrichment analysis (GSEA) for cell cycle and apoptosis pathways in STB-D3, STB-D4 and Vero E6 cells after SARS-CoV-2 WT infection. (F) Images of SARS-CoV-2 infected Vero E6 cells and eSTBs and representative immunofluorescence staining images of TUNEL cell apoptosis detection assay. White arrows point to apoptotic cells. (G) RNAseq signal of *HERV-K* and *HERV-FRD* in SARS-CoV-2 infected STB-D3 and STB-D4 and the mock controls. Library size is used to normalize the reads. (H) GO and KEGG analysis for shared upregulated and downregulated genes in SARS-CoV-2 infected STB-D3 and STB-D4. (I) Bubble plot for genes of SARS-CoV-2, monkey host factors *ACE2*, *TMPRSS2*, *CTSV*, *CTSL*, *CTSB*, innate immune response, TNF signaling pathway, interleukin signaling pathway and TNF-α/NF-κB signaling in Vero E6 after SARS-CoV-2 infection. Label color is according to z-score and bubble sizes are proportional to expression levels.

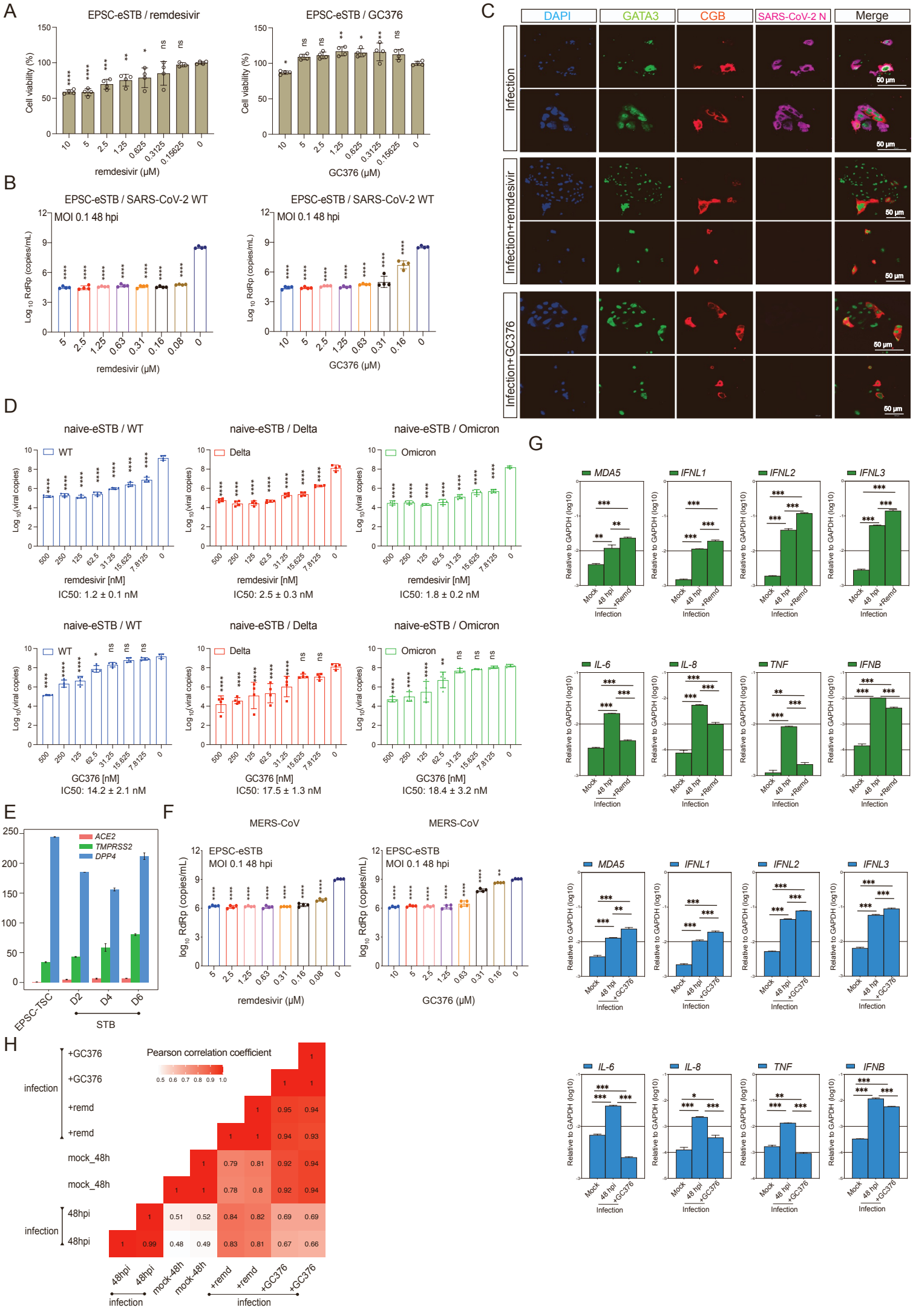
A
EPSC-eSTB / remdesivir
EPSC-eSTB / GC376
Cell viability (%)
remdesivir (μM)
GC376 (μM)
B
EPSC-eSTB / SARS-CoV-2 WT
MOI 0.1 48 hpi
Log10 RdRp (copies/mL)
C
DAPI
GATA3
CGB
SARS-CoV-2 N
Merge
Infection
Infection+remdesivir
Infection+GC376
50 μm
D
naive-eSTB / WT
naive-eSTB / Delta
naive-eSTB / Omicron
Log10(viral copies)
remdesivir [nM]
IC50: 1.2 ± 0.1 nM
IC50: 2.5 ± 0.3 nM
IC50: 1.8 ± 0.2 nM
GC376 [nM]
IC50: 14.2 ± 2.1 nM
IC50: 17.5 ± 1.3 nM
IC50: 18.4 ± 3.2 nM
E
ACE2
TMPRSS2
DPP4
cpm
EPSC-TSC
D2
D4
D6
STB
F
MERS-CoV
EPSC-eSTB
MOI 0.1 48 hpi
log10 RdRp (copies/mL)
remdesivir (μM)
GC376 (μM)
G
MDA5
IFNL1
IFNL2
IFNL3
IL-6
IL-8
TNF
IFNB
Relative to GAPDH (log10)
Mock
48 hpi
+Remd
+GC376
Infection
H
Pearson correlation coefficient
+GC376
+remd
mock_48h
48hpi
infection

Figure S5. eSTBs for evaluating antiviral drugs in SARS-CoV-2 and MERS-CoV infection. Related to Figure 5. (A) Measurement of eSTB cell viability by a CellTiter-Glo assay kit upon remdesivir or GC376 treatment for 48 hours. The results are shown as % of the non-treated cells (mean ± SEM). Statistics analysis by two-tailed unpaired Student's *t*-test. (B) Viral load reduction assay was performed to evaluate the inhibitory effect of remdesivir and GC376 against SARS-CoV-2 WT infection in EPSC-eSTBs. Data are mean ± SEM, One-way ANOVA. (**** $P<0.0001$) (C) Immunofluorescence-stained eSTB for nucleus (Blue), GATA3 (Green), CGB (Red), and SARS-CoV-2 N protein (purple). eSTB infected by SARS-CoV-2 with or without remdesivir (10μM) /GC376 (10μM) treatment, respectively. (Scale bar, 50 μm). (D) Viral load reduction assay for evaluating the inhibitory effect of the indicated drugs against SARS-CoV-2 WT and Delta and Omicron variants infection in naïve-eSTB cells. (E) Barplot for expression (cpm) of *ACE2*, *TMPRSS2* and *DPP4* in EPSC-TSC and EPSC-TSC differentiation toward STB. (F) Viral load reduction assay for evaluating the inhibitory effect of the indicated drugs against MERS-CoV infection in EPSC-eSTBs. (G) RT-qPCR detection of *MDA5*, *IFNLs, IL6*, *IL8*, *TNF* and *IFNB* in SARS-CoV-2 infected EPSC-eSTBs, in the presence or absence of remdesivir or GC376. Data are normalized to *GAPDH* using ΔCt, mean ± s.d. n=3. Student's *t*-test, *** $P<0.001$, ** $P<0.01$,* $P<0.05$ (H) Heatmap for correlation between infected and mock infection EPSC-eSTBs. Non-expressed genes were filtered out and cpm was used to calculate the Pearson correlation coefficient.

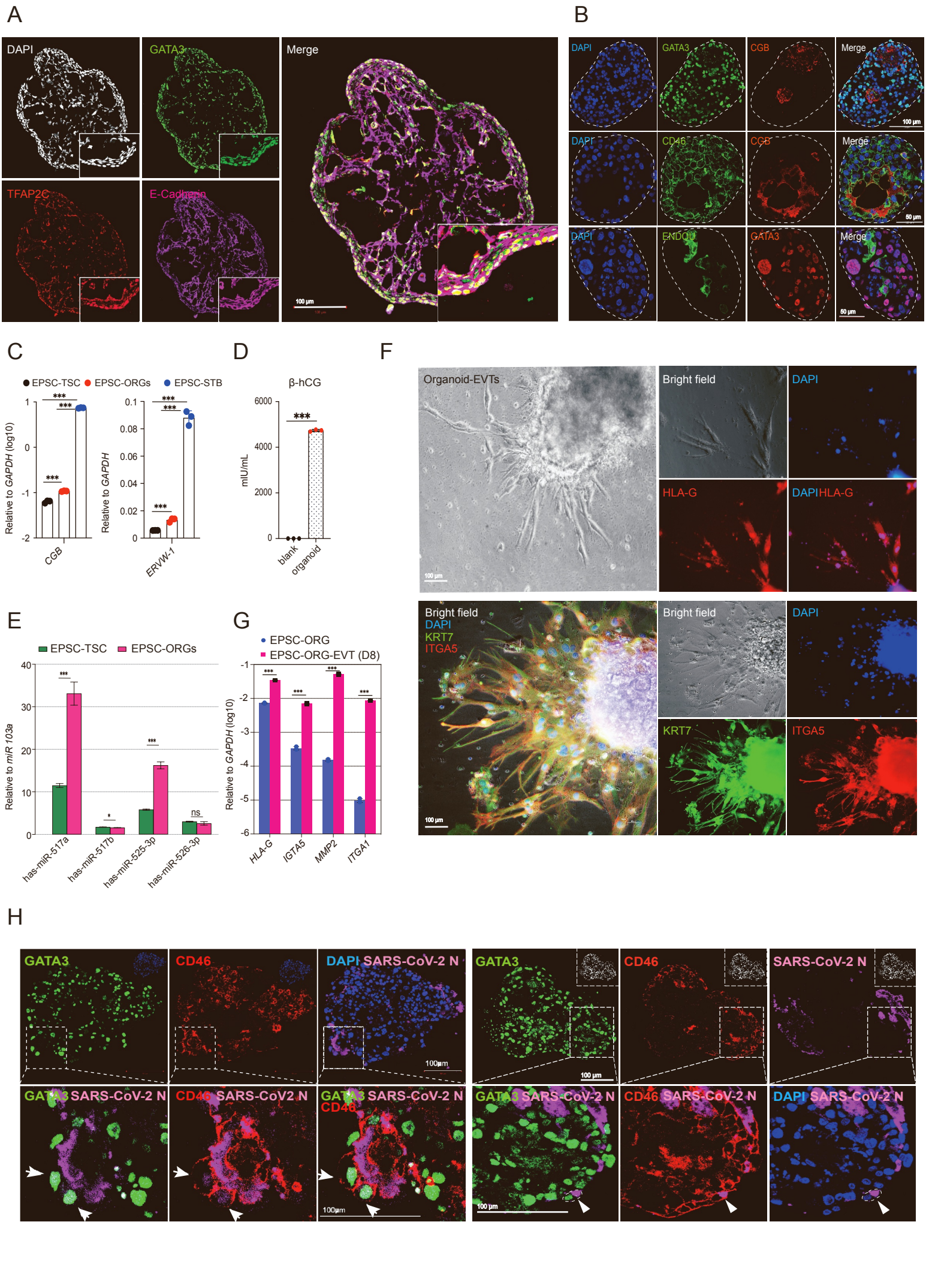
A
DAPI
GATA3
Merge
TFAP2C
E-Cadherin
100 μm
B
DAPI
GATA3
CGB
Merge
100 μm
DAPI
CD46
CGB
Merge
50 μm
DAPI
ENDOU
GATA3
Merge
50 μm
C
EPSC-TSC
EPSC-ORGs
EPSC-STB
Relative to GAPDH (log10)
CGB
Relative to GAPDH
ERVW-1
D
β-hCG
mIU/mL
blank
organoid
F
Organoid-EVTs
Bright field
DAPI
HLA-G
DAPI HLA-G
100 μm
Bright field
DAPI
KRT7
ITGA5
100 μm
Bright field
DAPI
KRT7
ITGA5
E
EPSC-TSC
EPSC-ORGs
Relative to miR 103a
has-miR-517a
has-miR-517b
has-miR-525-3p
has-miR-526-3p
ns
G
EPSC-ORG
EPSC-ORG-EVT (D8)
Relative to GAPDH (log10)
HLA-G
IGTA5
MMP2
ITGA1
H
GATA3
CD46
DAPI SARS-CoV-2 N
100μm
GATA3
CD46
SARS-CoV-2 N
100 μm
GATA3 SARS-CoV-2 N
CD46 SARS-CoV2 N
GATA3 SARS-CoV-2 N
CD46
100μm
GATA3 SARS-CoV-2 N
CD46 SARS-CoV-2 N
DAPI SARS-CoV-2 N
100 μm

Figure S6. Infection of EPSC-TSC-derived trophoblast organoids by SARS-CoV-2. Related to Figure 6. (A) Immunofluorescence-stained trophoblast organoid cryosections for TFAP2C, GATA3 and E-cadherin. Scale bar: 100 μm (B) Immunofluorescence-stained trophoblast organoid paraffin sections for CD46, GATA3, ENDOU and CGB. (C) Expression of STB genes in STBs, EPSC-TSCs and trophoblast organoids by RT-qPCR (mean ± s.d. n=3). Student's *t*-test. *** $P<0.001$ (D) ELISA (mIU/mL) detection of hCG-β secreted by trophoblast organoids in the supernatant. Fresh TOM was used as the blank control. n=3 independent replicates. *** $P < 0.001$ (Student's *t*-test). (E) Expression changes (RT-qPCR) of Trophoblast-specific C19MC miRNAs in EPSC-TSCs and trophoblast organoids. *miRNA103a* expression is used as the control. Data are mean ± s.d., n=3. (F) Representative phase-contrast image of cells migrating out of a trophoblast organoid seeded in EVT medium for 8 days. EVTs were stained for HLA-G, ITGA5 and KRT7. Nuclei were counterstained with DAPI. (G) EVT genes expression (RT-qPCR) in trophoblast organoids and trophoblast organoid-derived EVTs. Data are mean ± s.d. n=3. Student's *t*-test, *** $P < 0.001$ (H) Additional immunofluorescence-stained SARS-CoV-2-infected trophoblast organoid paraffin sections for GATA3, CD46 and SARS-CoV-2-N. Arrows indicate an infected cell that is co-stained for GATA3, CD46 and SARS-CoV-2-N. Scale bar: 100 μm

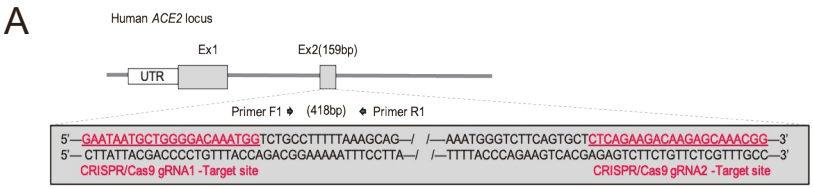

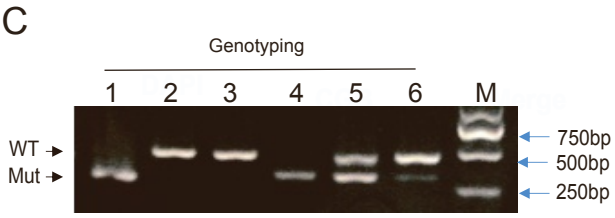

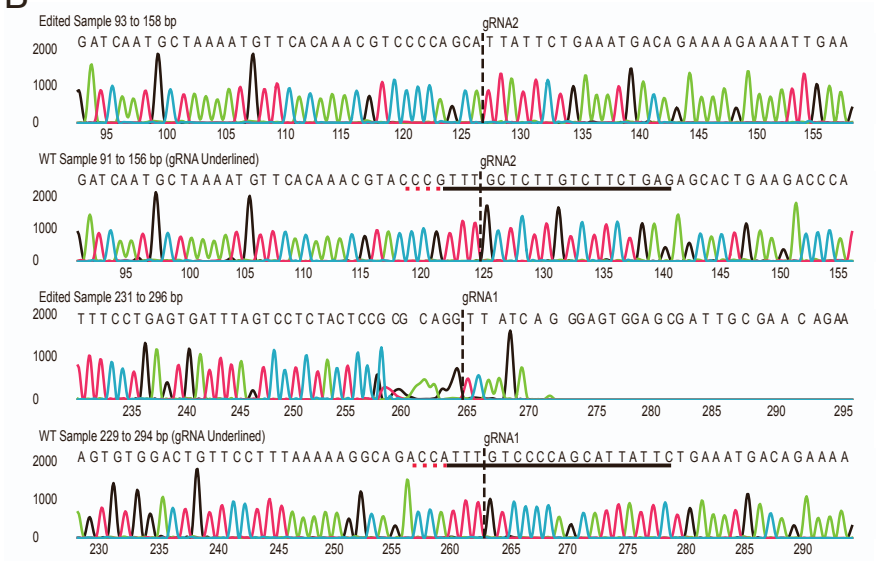

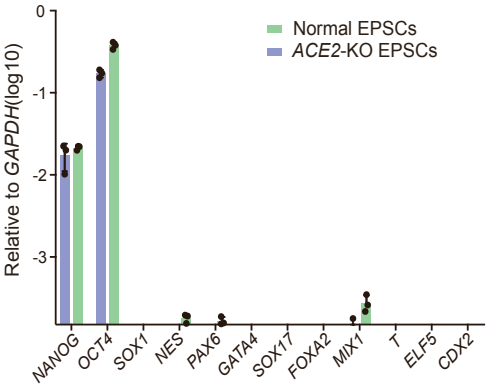

Sanger sequencing

wildtype 5'—GTTCACAAACGTACCCGTTTGCTCTTG--//--GGCAGACCATTCCCCAGCATTATTCTGAAAT—3'
Knock-out 5'—GTTCACAAACGT----------(148bp)----------CCCCAGCATTATTCTGAAAT—3'

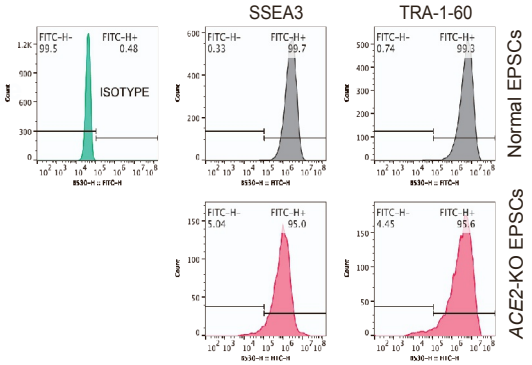

D

summary of *ACE2* Knock-out in EPSCs

cell line	no.of picked single clones	no. of genotyped	no. of heterozygote	no. of homozygote
M1 EPSCs	24	24	4	5

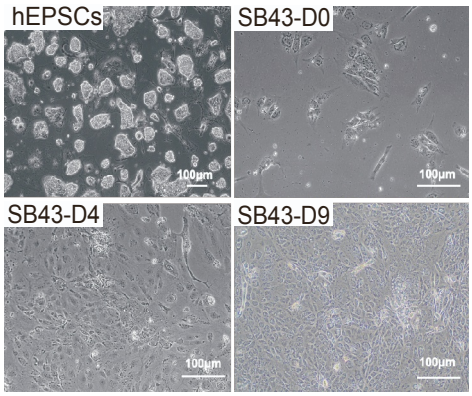

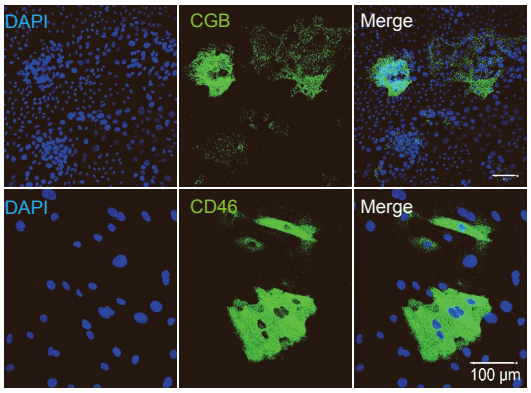

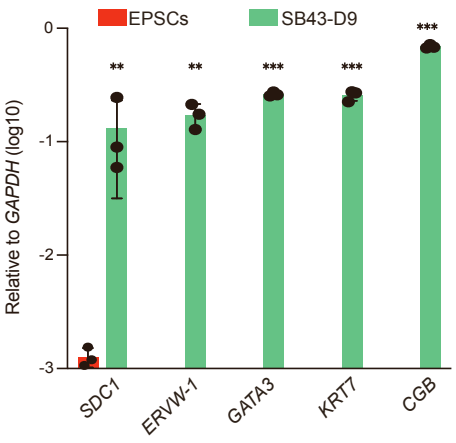

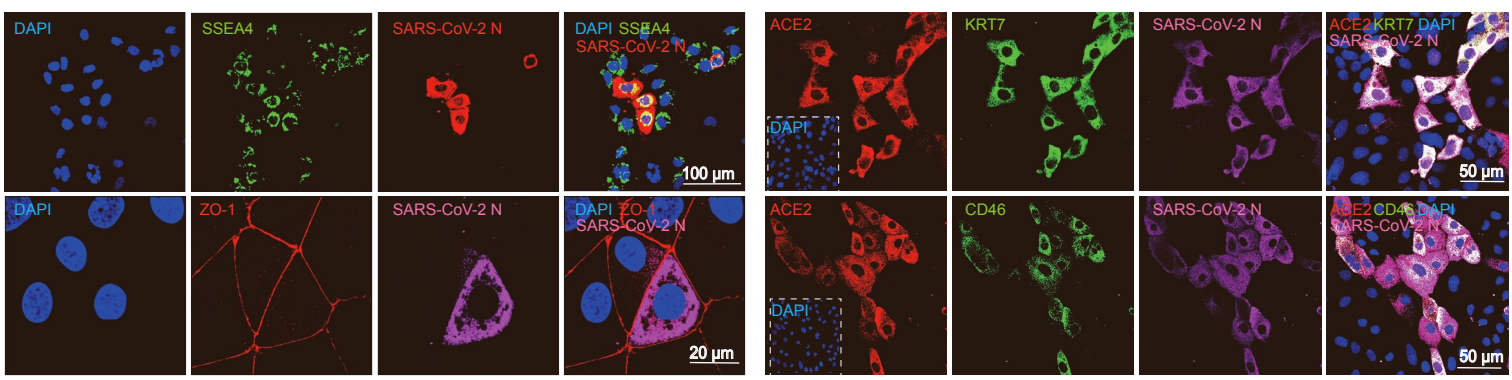

Figure S7. ACE2 is required for SARS-CoV-2 infection of human trophoblasts differentiated from hEPSCs. Related to Figure 7. (A) CRISPR/Cas9-mediated knockout of the human *ACE2* gene. A pair of gRNAs targeting exon 2 of *ACE2* are listed in red. (B) Sanger sequencing of the mutant PCR fragment reveals a 148 bp deletion between the two CRISPR gRNAs in exon 2 as expected. (C) Genotyping of *ACE2*-KO hEPSC colonies by genomic DNA PCR. Colonies 1 and 4 are homozygous KO mutants. (D) Genome editing efficiency at the *ACE2* locus in hEPSCs. (E) Expression of pluripotency and various cell lineage genes in normal and *ACE2*-KO hEPSCs. (F) Flow cytometry quantification of pluripotency markers SSEA3 and TRA-1-60 on normal and *ACE*2-KO hEPSCs. (G) Morphology of hEPSCs and SB43-treated cells on days 0, 4 and 9. Scale bars: 100 μm (H) Immunofluorescence staining images of STB markers CGB and CD46 in SB43-treated hEPSCs on day 9. Scale bars: 100 μm (I) Expression of trophoblast genes in SB43-treated hEPSCs on day 9 by RT-qPCR. Data are mean ± s.d. n=3. Student's *t*-test. (J) Immunofluorescence images of SARS-CoV-2 infection in SB43-treated hEPSCs (day 4). More mono- and bi-nucleated cells were infected. Scale bar: 50 μm and 100 μm as indicated.

Table S2. Culture conditions for hTSCs from different reports, Related to Figure 1.

Cell Type	CO2 and O2	ECM	TSCM modification 1	TSCM modification 2	TSCM modification 3	TSCM modification 4	Reference
TSC-BST/ct	5% CO2	Collagen IV	0.5 uM A83-01	1uM SB431542	1.5 ug/ml L-ascorbic acid	0.8 mM VPA	Okae, H., et al. (2018)
Primed-TSC	5% CO2	Matrigel	0.5 uM A83-01	1uM SB431542	1.5 ug/ml L-ascorbic acid	0.8 mM VPA	Wei, Y., et al. (2021)
Naïve-TSC (PXGL)	7% CO2 and 5% O2	Collagen IV/ MEF	1.0 uM A83-01	Without SB431542	1.5 mg/ml L-ascorbic acid	0.8 mM VPA	Guo, G., et al. (2021)
Naïve-TSC (5iLA)	5% CO2 and 20% O2	Collagen IV	0.5 uM A83-01	1uM SB431542	1.5 ug/ml L-ascorbic acid	0.8 mM VPA	Dong, C., et al. (2020)
EPSC-TSC	5% CO2	Geltrex	0.5 uM A83-01	1uM SB431542	50 ug/ml	10 uM VPA	This study

Table S3. Correlation index between ACE2 and Trophoblast markers, Related to Figure 2.

Gene	coefficient	*P* value
CDX2	0.04266543	0.00256635
CD46	0.24451753	7.03E-69
TFRC	-0.0493468	0.00048636
GCM1	-0.0636706	6.72E-06
CGB3	0.10253989	3.79E-13
CGB5	0.19950932	5.37E-46
SDC1	0.10222731	4.46E-13
GATA2	-0.0356747	0.01170267
GATA3	-0.0968373	7.03E-12
TP63	-0.0269452	0.05692952
TEAD4	-0.1328758	4.15E-21
ACE2	1	0
ENG	0.20688926	2.11E-49
ITGA5	0.10266201	3.55E-13
ITGA6	-0.0676585	1.71E-06
CSH1	0.18957838	1.27E-41
CSH2	0.24808141	6.54E-71
HLA-G	0.0706351	5.85E-07
MMP2	0.03941273	0.00534726

Table S5. List of PCR primers, Related to Figure 1, 4, 6, 7, S1, S3, S5-7.

Gene Name	Forward (5'-3')	Reverse (5'-3')
SARS-CoV-2	CGCATACAGTCTTRCAGGCT	GTGTGATGTTGAWATGACATGGTC
ACE2 (Exon9-10)	TCCATTGGTCTTCTGTCACCCG	AGACCATCCACCTCCACTTCTC
TMPRSS2	CTCTACGGACCAAACTTCATC	CCACTATTCCTTGGCTAGAGTA
CD147	GGCTGTGAAGTCGTCAGAACAC	ACCTGCTCTCGGAGCCGTTCA
NANOG	TGAACCTCAGCTACAAACAG	TGGTGGTAGGAAGAGTAAAG
Oct-04	CCTCACTTCACTGCACTGTA	CAGGTTTTCTTTCCCTAGCT
SOX2	TTCACATGTCCCAGCACTACCAGA	TCACATGTGTGAGAGGGGCAGTGTGC
CDX2	TTCACTACAGTCGCTACATCACC	TTGATTTTCCTCTCCTTTGCTC
GATA3	ACATCTCGCCCTTCAGCCAC	CATGGCGGTGACCATGCTGGA
KRT7	AGGATGTGGATGCTGCCTAC	CACCACAGATGTGTCGGAGA
TEAD4	CAGGTGGTGGAGAAAGTTGAGA	GTGCTTGAGCTTGTGGATGAAG
TFAP2C	ACAGGATCCATGTTGTGGAAAATAACCGAT	ATACTCGAGTTTCCTGTGTTTCTCCATTTT
TP63	AGAAACGAAGATCCCCAGATGA	CTGTTGCTGTTGCCTGTACGTT
CGB	ACCCTGGCTGTGGAGAAGG	ATGGACTCGAAGCGCACA
ERVW-1	GTTAATGACATCAAAGGCACCC	CCCCATCTCAACAGGAAAACC
SDC1	GCTGACCTTCACACTCCCCA	CAAAGGTGAAGTCCTGCTCCC
HLA-G	CAGATACCTGGAGAACGGGA	CAGTATGATCTCCGCAGGGT
MMP2	TGGCACCCATTTACACCTACAC	ATGTCAGGAGAGGCCCCATAGA
ITGB6	CTCAACACAATAAAGGAGCTGGG	AAAGGGGATACAGGTTTTTCCAC
GABRP	TTTCTCAGGCCCAATTTTGGT	GCTGTCGGAGGTATATGGTGG
MUC16	GGAGCACACGCTAGTTCAGAA	GGTCTCTATTGAGGGGAAGGT
VTCN1	TCTGGGCATCCCAAGTTGAC	TCCGCCTTTTGATCTCCGATT
cGAS	TAACCCTGGCTTTGGAATCAAAA	TGGGTACAAGGTAAAATGGCTTT
ZBP1	TGGTCATCGCCCAAGCACTG	GGCGGTAAATCGTCCATGCT
MDA5	GAGCAACTTCTTTCAACCACAG	CACTTCCTTCTGCCAAACTTG

STING1	AGCATTACAACAACCTGCTACG	GTTGGGGTCAGCCATACTCAG
IFNA2	CTTGAAGGACAGACATGACTTTGGA	GGATGGTTTCAGCCTTTTGGA
IFNB1	AAACTCATGAGCAGTCTGCA	AGGAGATCTTCAGTTTCGGAGG
IFNG	TGGCTTTTCAGCTCTGCATC	CCGCTACATCTGAATGACCTG
IFNL1	CGCCTTGGAAGAGTCACTCA	GAAGCCTCAGGTCCCAATTC
IFNL2	AGTTCCGGGCCTGTATCCAG	GAGCCGGTACAGCCAATGGT
IFNL3	TCGCTTCTGCTGAAGGACTGCA	CCTCCAGAACCTTCAGCGTCAG
IFNL4	ATGCGGCCGAGTGTCTGG	GCTCCAGCGAGCGGTAGTG
IL6	GTCAGGGGTGGTTATTGCAT	AGTGAGGAACAAGCCAGAGC
IL28A	TCCAGTCACGGTCAGCA	CAGCCTCAGAGTGTTTCTTCT
TNF	CTCTTCTGCCTGCTGCACTTTG	ATGGGCTACAGGCTTGTCACTC
HLA-A	CGAGGATGGCCGTCATGGCG	CACATTCCGTGTCTCCTGGTCCC
HLA-B	CAGTTCGTGAGGTTCGACAG	CAGCCGTACATGCTCTGGA
ITGA1	CTGGACATAGTCATAGTGCTGGA	ACCTGTGTCTGTTTAGGACCA
ITGA5	GTCGGGGGCTTCAACTTAGAC	CCTGGCTGGCTGGTATTAGC
ITGA6	CACATCTCCTCCCTGAGCAC	TATCTTGCCACCCATCCTTG
CDX2	TTCACTACAGTCGCTACATCACC	TTGATTTTCCTCTCCTTTGCTC
ELF5	TGCCCTCACGGTAATGTTGGA	TGATGCTCAAAGGCAGGGTAG
GAPDH	CAAATTCCATGGCACCGTCA	ATCGCCCCACTTGATTTTGG
human miR-103a	GTAGCAGCATTGTACAGGG	
human miR-526b-3p	GTTTGGGAAAGTGCTTCCTTTT	
human miR-517a	GTTTGGATCGTGCATCCTTTTA	
human miR-517b	GTGCCTCTAGATGGAAGCA	
human miR-525-3p	GTTGAAGGCGCTTCCCTTT	